

Applications of Wireless Sensor Network for Monitoring System Based on IOT

Wen-Tsai Sung*, Jui-Ho Chen, Ming-Han Tsai

Electrical Engineering Department, National Chin-Yi University of Technology, Taiwan,
No.57, Sec. 2, Zhongshan Rd., Taiping Dist., Taichung 41170, Taiwan
(*e-mail: songchen@nct.edu.tw).

Abstract—A number of ZigBee based monitoring systems are built on the basis of IOT technology in this work on the perception layer, using temperature/humidity sensors, light sensors and 3-axis accelerometer modules. Wirelessly transmitted to a monitoring center, all the sensed data are collected by a human computer interface. On the application layer in an IOT, simulation experiments are conducted, namely, applications of light sensors to an automated basketball court lighting system, 3-axis accelerometer modules to the monitoring of infant's sleeping posture and accidental fall of the elderly, and temperature/humidity sensors to thermal comfort testing. This research work is validated as an effective way to achieve the aim of power consumption reduction, improve the health care quality and provide a higher comfort level.

Index Terms—Wireless Sensor Network, ZigBee, IOT, Quantum Particle Swarm Optimization, Sensors.

I. INTRODUCTION

An Internet of Things (IOT) refers to a network where objects treated as sensing nodes are all connected for long distance wireless data communication by the use of the key radio frequency identification (RFID) technique and a wireless sensors network (WSN) [1-3], there are a total of 3 layers in an IOT architecture, namely, perception layer, network layer and application layer [4]. Involving RFID, WSN, sensors, readers, IP Cam, MEMS, etc. [5], the perception layer at the bottom is the layer that takes charge of data collection and object identification. It can be perceived as the sensory organs in a human body, i.e. the only means of communication from the environment to the nervous system, such as eyes, nose, mouth, ears, and the like.

As the middle layer, the network layer serves as the data link communication system, just as the nervous system for signal delivery, between devices or even devices/humans. Composed of an IOT data management center, 2G/3G, Wi-Fi, WiMAX, ZigBee, etc. and with multi-node for extended transmission ranges, it can be merged with other local area networks into a larger one as an enhanced service provider. As its name indicates, the top layer, referred to as the application layer, is devoted to a diversity of practical applications, e.g. the commonly seen environment monitoring, smart home systems, health care, etc. The application support layer, a sub application layer, is developed for data processing in supported platforms,

including open source information, cloud computing and service support platforms. In this manner, various platforms are integrated for a wide range of services so as to elevate the use frequency of an IOT. Covering a great number of research fields, the framework of an IOT is made up of perceived control layer, network transport layer and application service layer. [6-9]

II. SYSTEM ARCHITECTURE AND HARDWARE DEVELOPMENT PLATFORM

As illustrated in Fig. 1, a monitoring system is constructed using a wireless sensor network with a CC2530 ZigBee development kit and through RFID technology in this study. The adopted IOT perception layer technology cover WSM, sensors, RFID and reader, responsible for data collection and recognition, while a ZigBee module mainly takes charge of wireless data communication in perception layer. The application layer, the top of an IOT, is in charge of environment lighting control and thermal comfort monitoring, and the support layer thereof analyzes the sensed data through a particle swarm optimization algorithm. [10-18] There are star and symmetrical topologies in an IEEE 802.15.4-based wireless sensor network. Hence, a star topology is adopted to implement a ZigBee wireless network. There are seven sensing nodes deployed for data collection, i.e. a full-function device (FFD) and 6 reduction-function devices (RFDs). The only FFD serves as the critical points, while the remaining six RFDs act as terminals devices, namely perception layer technology member, including temperature/humidity, light, 3-axis accelerometer sensors, 125 KHz LF, 13.56 MHz HF, 900 MHz UHF and 2.45 GHz microwave RFID readers. The ZigBee network in this work is composed of a SmartRF05EB board, 7 battery powered SmartRF05BB boards, 3 sensors and 4 RFID modules. Each piece of collected data is routed toward the critical points, displayed and then processed in a PC. [19-22]

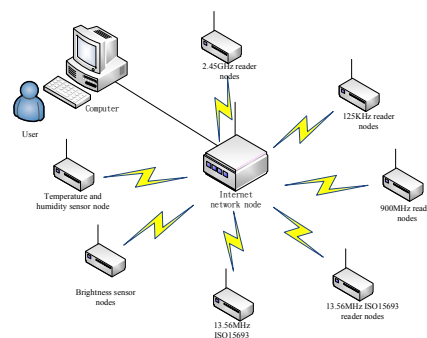


Fig. 1. Constituents of the proposed ZigBee-based monitoring system.

III. SUFFICIENT OUTDOOR LIGHTING EXPERIMENT AND ANALYSIS

This work employs a photoresistor MJ5516 as a light sensor to conduct an outdoor lighting simulation experiment. In compliance with CNS lighting standard, the light sensor is applied to the control of street, stadium and parking lot lights. For instance, the basketball court lighting is monitored and controlled, and data are transmitted among members of the network layer in an IOT. The lighting status sensed are transmitted in a ZigBee network, displayed on a GUI as a bar graph, and then saved in real time.

As illustrated in Fig. 2, the outdoor basketball court lighting ranges between 75 and 1500 Lux in compliance with CNS lighting standard. For most sporting events, an illuminance of 450 Lux, i.e. 30% of 1500 Lux, is recommended and indicated by a green indicator, while in case below 30%, an outdoor lighting facility is switch on to provide adequate illuminance. The sensed illuminance is delivered by ZigBee technique and received by a remote GUI. An average illuminance above 80% is observed in a sufficient outdoor light level, and 30% is treated as a threshold to switch on the outdoor lighting facility.

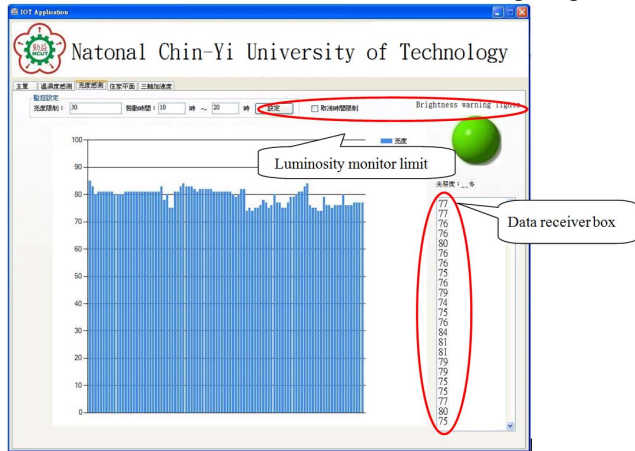


Fig. 2. An illustration of sufficient outdoor lighting.

IV. INFANTS AND ELDERLY CARE EXPERIMENT AND ANALYSIS

A 3-axis accelerometer module is adopted in this simulation experiment with infants and the elderly as test objects. Either the sleeping postures or the accidental fall of the test objects, identified by RFID technology, are monitored by body-mounted accelerometer modules. The 3-axis acceleration signals, transmitted by ZigBee technique, are plotted against time on a GUI, and the real time data are listed at the bottom of the window which can be saved as a file. (see the Fig.3)

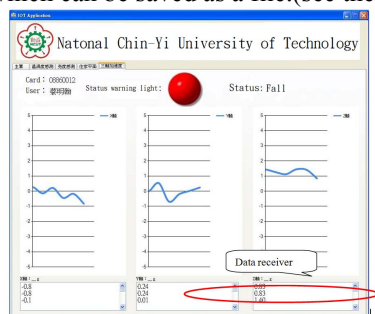


Fig. 3. An illustration of 3-axis acceleration data presentation on a GUI.

A. Lying state

As illustrated in Fig. 4, accelerations of 0, 0 and 1.5g in the x, y and z axes respectively represent a lying state.

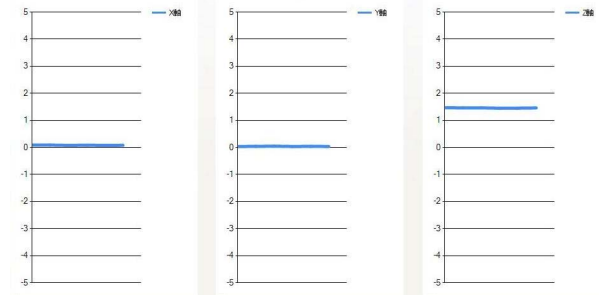


Fig. 4. Acceleration signals in a lying state along the x, y and z axes.

B. Lying on right and left side

As illustrated in Fig. 5, a lying state, either on left or right side, is identified using the x-axis acceleration signal. In Fig. 7(a), a rise from 0 to 1g acceleration in the x-axis denotes the transition between a lying state and that on the right side. In contrast, a smooth signal drop from 0 to -1g represents the movement from a lying state to that on the left side.

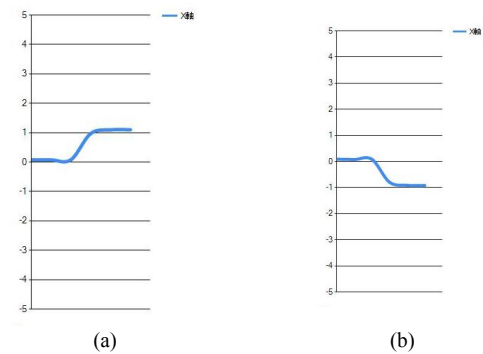


Fig. 5. Acceleration signals when lying on (a) right and (b) left side along the x, y and z axes.

C. Lying sleeping state

As illustrated in Fig. 6, a free falling sleep position is identified by a z-axis signal. A comparison between Fig. 8(a) and 8 (b) reveals consistent z-axis signals, and a rise and a drop in the x- and y-axis signals indicate movements from a lying state on right side to free faller and that from a lying state on right side to free faller, respectively.

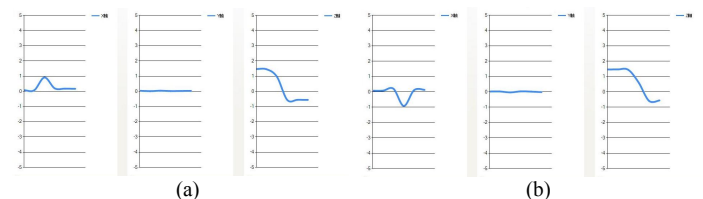


Fig. 6. Acceleration signals during the transition (a) from the left side and (b) from the right side to a free falling sleep position along the x, y and z axes.

V. ENVIRONMENTAL COMFORT LEVEL MONITORING EXPERIMENT AND ANALYSIS

In this case, a simulation experiment is conducted by use of a SHT10 temperature humidity sensor module. Adopted by the Central Weather Bureau, Taiwan, the thermal comfort level [23] is expressed as

$$\alpha = \beta - 0.55 \left[1 - \frac{\exp\left(\frac{r \cdot 17.269}{237.30 + \gamma}\right)}{\exp\left(\frac{\beta \cdot 17.269}{237.30 + \beta}\right)} \right] \cdot (\beta - 14) \quad (1)$$

$$\gamma = \frac{\beta \cdot \phi}{100} \quad (2)$$

where α denotes the comfort index in °C, β the temperature, ϕ the relative humidity, and γ the dew point.

As tabulated in Table 1 [23], the comfort level is divided into 6 levels. The dew point and then the comfort level are evaluated once the temperature/ humidity are specified in a Visual Basic program. Demonstrated in Fig. 12 is an illustration on the condition that $T = 21^\circ\text{C}$ and $rH = 50.6\%$.

TABLE 1 COMFORT LEVELS CORRESPONDING TO HUMAN PERCEPTION

| Comfort index (°C) | Comfort level |
|--------------------|---------------------|
| 10°C or less | Very cold |
| 11°C ~ 15°C | Cold |
| 16°C ~ 19°C | Cool slightly |
| 20°C ~ 26°C | Comfortable |
| 27°C ~ 30°C | Muggy |
| 31°C or above | Easy to heat stroke |

A. Ambient temperature and humidity difference compared

(a) Before environmental adaptation

This simulation experiment is conducted for a monitoring of comfort level. As illustrated in Fig. 7, the average outdoor temperature, issued by the Central Weather Bureau Taiwan on an hourly basis, is treated as a reference, while the indoor is

sensed by this proposed temperature monitoring system. A high temperature drop is found between the indoor and outdoor temperatures, giving rise to a low comfort level. Hence, there is a need to power on an air conditioner(s) to meet the recommended comfort level.

Both the temperature and the humidity are found to dominate the comfort level. The outdoor humidity is susceptible to multiple weather factors, e.g. rainfall, sunshine, etc, while a relatively low variation is seen in the indoor humidity, as illustrated in Fig. 8. In other words, indoor humidity can be well regulated as recommended by a humidifier/dehumidifier.

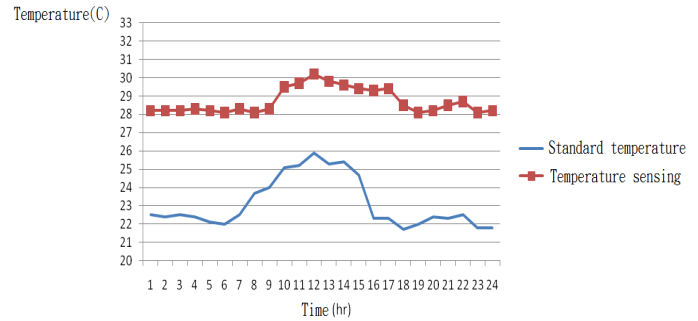


Fig. 7. A comparison between indoor and outdoor temperatures on an hourly basis.

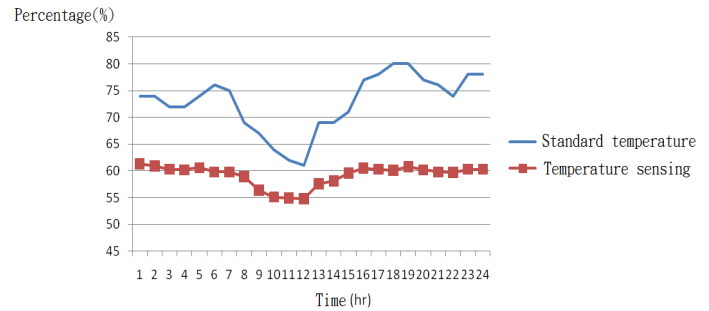


Fig. 8. A comparison between indoor and outdoor humidity on an hourly basis.

(b) After environmental adaptation

The proposed system targets a comfort level of 20-26 during the time period between 10:00 and 16:00. Demonstrated in Figs. 16,17, as opposed to Figs. 14-15, are the comparisons of outdoor versus regulated indoor temperature and relative humidity respectively. As can be found in Figs. 9-10, the indoor temperature and humidity starts to fall over time in an effort to meet intended comfort level since the operation of an air conditioner at 10:00.

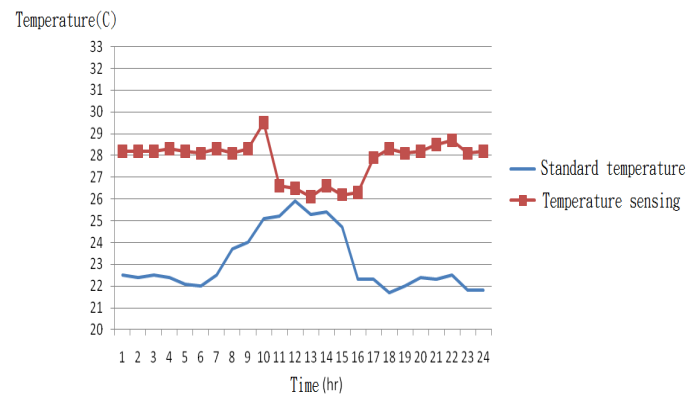


Fig. 9. A comparison between outdoor and regulated indoor temperatures on an hourly basis.

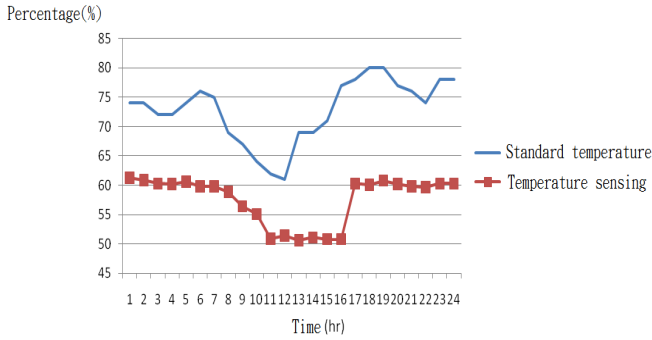


Fig. 10. A comparison between outdoor and regulated indoor humidity on an hourly basis. Presented in Fig. 11 is a comparison of outdoor / unregulated / regulated comfort levels versus time on an hourly basis. The outdoor comfort level indicates that it is a beautiful day for outdoor events, while the unregulated indoor one reveals a muggy weather condition. Hence, this proposed smart ZigBee-based monitoring system is validated as an effective way to reach recommended indoor comfort levels for household purpose.

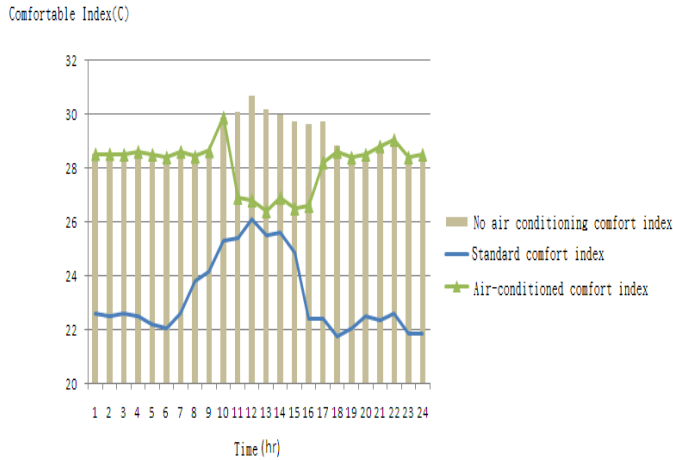


Fig. 11. A comfort level comparison among outdoor, indoor and air conditioning environments.

VI. QPSO ALGORITHM ANALYSIS

The QPSO algorithm is validated by the following 3 typical test functions, and an optimization comparison is made with a basic particle swarm optimization (BPSO) algorithm.

Sphere function:

$$f_1(x) = \sum_{i=1}^n x_i^2 \quad (3)$$

Peaks function:

$$f_2(x) = 3(1-x)^2 e^{-x^2-(y+1)^2} - 10\left(\frac{x}{5} - x^3 - y^5\right) e^{-x^2-y^2} - \frac{1}{3} e^{-(x+1)-y^2} \quad (4)$$

Schaffer's f_6 function:

$$f_3(x) = 0.5 + \frac{(\sin \sqrt{(x^2 + y^2)})^2 - 0.5}{[1.0 + 0.01(x^2 + y^2)]^2} \quad (5)$$

Tabulated in Table 3 are the fundamental features of the above typical test functions, among which both f_1 and f_2 are made for a minimum value problem, while f_3 is instead for a maximum value problem.

TABLE 3. RESPECTIVE FUNDAMENTAL FEATURES OF TEST FUNCTIONS.

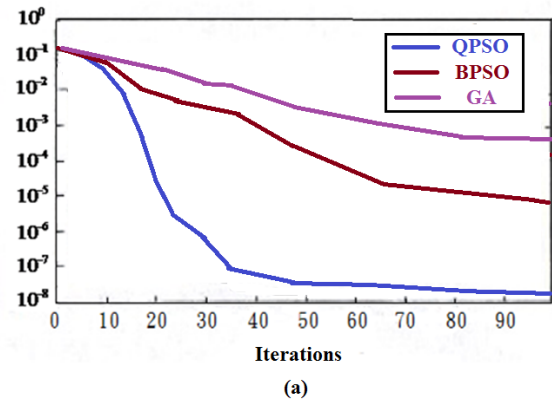
| Test function | Dimension | Search interval | Optimal extreme point | Optimal target |
|---------------|-----------|-----------------|-----------------------|----------------|
| f_1 | 2 | $[-5, 5]$ | $(0, 0)$ | 0 |
| f_2 | 2 | $[-3, 3]$ | $(0, 2)$ | 8 |
| f_3 | 2 | $[-5, 5]$ | $(0, 0)$ | 0 |

Letting the maximum number of iteration $T_{max} = 100$, the particle swarm size $n = 10$ and the Particle dimension $m = 2$, a performance measure is defined as

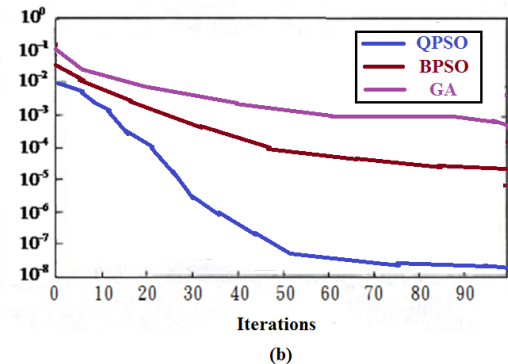
$$e = \frac{1}{n} \sqrt{\sum_{i=1}^n (x_i - \hat{x}_i)^2} \quad (6)$$

This performance measure reflects the error between the expected and the real output values. Presented in Fig. 12(a)~(c) are the comparison results of the error versus the iteration count among a BPSO algorithm, a QPSO algorithm and a genetic algorithm (GA). The QPSO is found superior to BPSO and GA in the aspects of optimization accuracy and fitness.

Error Sum of Squares



Error Sum of Squares



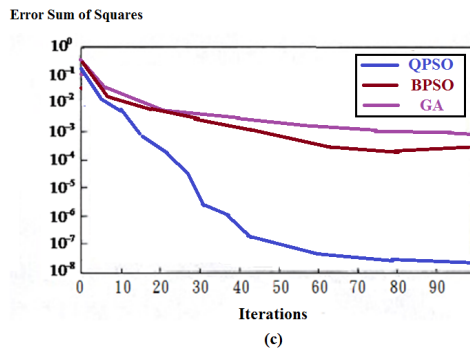


Fig. 12. comparison results of error accuracy versus iteration number among various algorithm with (a) Sphere, (b) Peaks and (c) Schaffer's f6 functions.

VII. CONCLUSION AND FUTURE WORKS

A 3-axis accelerometer module is employed as a body mounted device, in particular on the waist of such test objects as infants, the elderly and patients. In case of any urgent matters, e.g. dangerous sleeping positions for infants and accidental fall for the elderly, and so forth, monitored in a ZigBee network as well as displayed in a GUI, medical stuff are alerted immediately by a monitoring center for performing first aid on the test objects. In this manner, manpower shortage can be relieved, and the medical care quality can be boosted accordingly. Another issue addressed in this study is a long term monitoring of indoor temperature/humidity. Due to a multitude of collected data, a thermal comfort optimization problem is resolved by use of a QPSO algorithm. The analysis on the temperature/humidity is treated as a foundation for successive interior design and even modification.

REFERENCES

- [1] Wang, C.; Daneshmand, M.; Dohler, M.; Mao, X.; Hu, R.Q.; Wang, H., Guest Editorial - Special Issue on Internet of Things (IoT): Architecture, Protocols and Services, *IEEE Sensors Journal*, 13, 10, 2013, 3505 - 3510.
- [2] Kawamoto, Y.; Nishiyama, H.; Fadlullah, Z.M.; Kato, N., Effective Data Collection Via Satellite-Routed Sensor System (SRSS) to Realize Global-Scaled Internet of Things, *IEEE Sensors Journal*, 13, 10, 2013, 3645 - 3654.
- [3] Lazarescu, M.T., Design of a WSN Platform for Long-Term Environmental Monitoring for IoT Applications, *IEEE Journal on Emerging and Selected Topics in Circuits and Systems*, 3, 1, 2013, 45 - 54.
- [4] Kelly, S.D.T.; Suryadevara, N.K.; Mukhopadhyay, S.C., Towards the Implementation of IoT for Environmental Condition Monitoring in Homes, *IEEE Sensors Journal*, 13, 10, 2013, 3846 - 3853.
- [5] Yongsheng Ding; Yanling Jin; Lihong Ren; Kuangrong Hao, An Intelligent Self-Organization Scheme for the Internet of Things, *IEEE Computational Intelligence Magazine*, 8, 3, 2013, 41 - 53.
- [6] Huang, Yu-Kai; Pang, Ai-Chun; Hsiu, Pi-Cheng; Zhuang, Weihua; Liu, Pangfeng, Distributed Throughput Optimization for ZigBee Cluster-Tree Networks, *IEEE Transactions on Parallel and Distributed Systems*, 23, 3, 2012, 513 - 520.
- [7] Kim Seong Hoon; Kang Jeong Seok; Park Hong Seong; Kim Daeyoung; Kim Young-Joo, UPnP-ZigBee internetworking architecture mirroring a multi-hop ZigBee network topology, *IEEE Transactions on Consumer Electronics*, 55, 3, 2009, 1286 - 1294.
- [8] Shih Yuan-Yao; Chung Wei-Ho; Hsiu Pi-Cheng; Pang Ai-Chun, A Mobility-Aware Node Deployment and Tree Construction Framework for ZigBee Wireless Networks, *IEEE Transactions on Vehicular Technology*, 62, 6, 2013, 2763 - 2779.
- [9] Ha Young-Guk, Dynamic integration of zigbee home networks into home gateways using OSGI service registry, *IEEE Transactions on Consumer Electronics*, 55, 2, 2009, 470 - 476.
- [10] Park Wan-Ki; Han, I.; Park, Kwang-Roh, ZigBee based Dynamic Control Scheme for Multiple Legacy IR Controllable Digital Consumer Devices, *IEEE Transactions on Consumer Electronics*, 53, 1, 2007, 172 - 177.
- [11] Yen Li-Hsing; Law Yee Wei; Palaniswami, M., Risk-Aware Distributed Beacon Scheduling for Tree-Based ZigBee Wireless Networks, *IEEE Transactions on Mobile Computing*, 11, 4, 2012, 692 - 703.
- [12] Yang Po; Wu Wenyan; Moniri, M.; Chibelushi, C.C., Efficient Object Localization Using Sparsely Distributed Passive RFID Tags, *IEEE Transactions on Industrial Electronics*, 60, 12, 2013, 5914 - 5924.
- [13] Boaventura, A.J.S.; Carvalho, N.B., A Batteryless RFID Remote Control System, *IEEE Transactions on Microwave Theory and Techniques*, 61, 7, 2013, 2727 - 2736.
- [14] Chen Sung-Lin; Lin Ken-Huang, Characterization of RFID Strap Using Single-Ended Probe, *IEEE Transactions on Instrumentation and Measurement*, 58, 10, 2009, 3619 - 3626.
- [15] Lin, Liangkui; Xu, Hui; Xu, Dan; An, Wei; Xie, Kai, QPSO-based algorithm of CSO joint infrared super-resolution and trajectory estimation, *Journal of Systems Engineering and Electronics*, 22, 3, 2011, 405 - 411.
- [16] Yangguang Fu; Mingyue Ding; Chengping Zhou, Phase Angle-Encoded and Quantum-Behaved Particle Swarm Optimization Applied to Three-Dimensional Route Planning for UAV, *IEEE Transactions on Systems, Man and Cybernetics, Part A: Systems and Humans*, 42, 2, 2012, 511 - 526.
- [17] Lian, Guangyao; Huang, Kaoli; Chen, Jianhui; Gao, Fenggi, Optimization method for diagnostic sequence based on improved particle swarm optimization algorithm, *Journal of Systems Engineering and Electronics*, 20, 4, 2009, 899 - 905.
- [18] Fang Yao; Zhao Yang Dong; Ke Meng; Zhao Xu; Iu, H.H.; Wong Kit Po, Quantum-Inspired Particle Swarm Optimization for Power System Operations Considering Wind Power Uncertainty and Carbon Tax in Australia, *IEEE Transactions on Industrial Informatics*, 8, 4, 2012, 880 - 888.
- [19] Li, F.; Xiong, P., Practical Secure Communication for Integrating Wireless Sensor Networks Into the Internet of Things, *IEEE Sensors Journal*, 13, 10, 2013, 3677 - 3684.
- [20] Munoz-Organero, M.; Ramiez-Gonzalez, G.A.; Munoz-Merino, P.J.; Delgado Kloos, C., A Collaborative Recommender System Based on Space-Time Similarities, *IEEE Pervasive Computing*, 9, 3, 2010, 81 - 87.
- [21] Raza, S.; Shafagh, H.; Hewage, K.; Hummen, R.; Voigt, T., Lithe: Lightweight Secure CoAP for the Internet of Things, *IEEE Sensors Journal*, 13, 10, 2013, 3711 - 3720.
- [22] Ganz, F.; Barnaghi, P.; Carrez, F., Information Abstraction for Heterogeneous Real World Internet Data, *IEEE Sensors Journal*, 13, 10, 2013, 3793 - 3805.
- [23] SENSIRION The Sensor Company, Datasheet SHT1x (SHT10, SHT11, SHT15) Humidity and Temperature Sensor IC, Version 5, December 2011.